Interrogation of fiber gratings by use of low-coherence spectral interferometry of noiselike pulses

Shay Keren and Moshe Horowitz

Department of Electrical Engineering, Technion—Israel Institute of Technology, Haifa 32000, Israel

Received July 10, 2000

We demonstrate an innovative method for a real-time interrogation of fiber Bragg gratings based on low-coherence spectral interferometry of noiselike pulses. By analyzing the spectral interference at the output of a Michelson interferometer we obtained the impulse response of the grating with a time resolution of ~350 fs. Using the Gabor transformation, we could directly detect nonuniform regions inside the grating and could measure the spatial dependence of the resonance wavelength along the grating. © 2001 Optical Society of America

OCIS codes: 060.2340, 050.2770.

Fiber Bragg gratings are important for various applications in optical communication systems and in optical metrology.[1] Novel methods for measuring the performance of complex gratings were recently demonstrated (see, for example, Ref. 2). Low-coherence-time reflectometry has been used to measure the impulse response of gratings.[3,4] However, because of the presence of photons that are multiply scattered and because of changes in the coherence properties of a wave that propagates inside the grating, the impulse response does not directly give the spatial distribution of the grating parameters. Low-coherence reflectometry performed in the frequency domain does not require a slow mechanical scan, as is needed in the time domain. This technique has been used with ultrafast pulses to measure the group-velocity dispersion of optical elements[5,6] as well as to measure the thickness of cover glasses by use of a multimode continuous wave laser.[7]

We used low-coherence spectral reflectometry of noiselike pulses to study the structure of fiber Bragg gratings. By analyzing the interference spectra, using Fourier and Gabor transformations, we found the impulse response of the grating and the grating's response to short pulses with different central frequencies. We used the Gabor transformation to find directly the spatial dependence of the resonance frequency of the grating and to detect nonuniform regions inside the grating. Our measurement technique requires in principle only a single pulse to permit us to measure the whole structure of the grating, and the technique can be important in the manufacture of complex chirped fiber gratings as well as for interrogating distributed fiber Bragg sensors.

In our measurements we used a laser that generates noiselike pulses.[8–11] Such a laser generates pulses with broader spectra and higher energies than those obtained in the conventional pulsed mode in the same laser cavity.[8,9] Noiselike pulses had been used previously to interrogate an array of fiber gratings with different resonance wavelengths.[10] The spatial resolution of the measurement was determined by the pulse duration (nanoseconds). Using the technique described in this Letter, we could increase the spatial resolution of the measurement to the order of the effective coherence length of our system (≈40 μm).

Figure 1 is a schematic diagram of the experimental setup. Our low-coherence source was a passively mode-locked erbium-doped fiber laser that generates noiselike pulses with an average power of 20 mW, a spectrum width of as much as 70 nm, a pulse duration of 2 ns, and a repetition rate of ~10 MHz. The laser output was split by a coupler. Part of the laser beam that was reflected from the grating interfered with another part of the beam that was reflected by a mirror. The optical paths of the two reflected beams were chosen to be similar but not equal, as explained below. A polarization controller was used to produce equal polarization states of the two interfering pulses. Figure 2 shows a typical interference spectrum measured for a nearly uniform grating with the reflection spectra shown in Fig. 3(a). Because the wave that is reflected from the grating interferes with a strong reference wave that is reflected by a mirror, the intensity of the interference component becomes significantly stronger than the intensity of the wave that was reflected by the grating. Therefore we were able to measure the interference spectrum far outside the Bragg zone of the grating, as shown in Fig. 2. The speed of our measurement was limited by the sweep time of the spectrum analyzer, 0.5 s, that we used to measure the interference spectrum. In principle, we need only a single pulse to map the whole grating. Therefore the

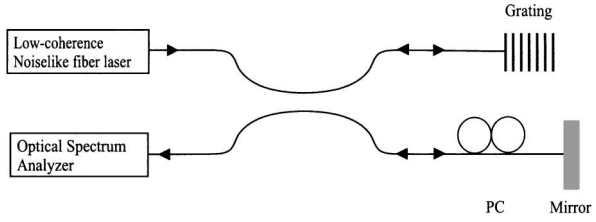

Fig. 1. Schematic diagram of the experimental setup: PC, polarization controller.

0146-9592/01/060328-03$15.00/0

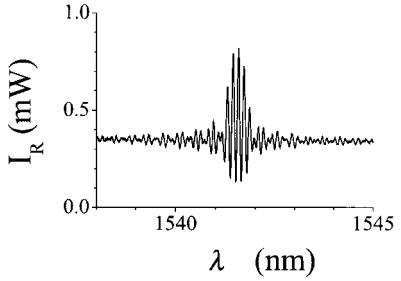

Fig. 2. Typical interference spectrum measured for a nearly uniform grating with the reflection spectrum shown in Fig. 3(a).

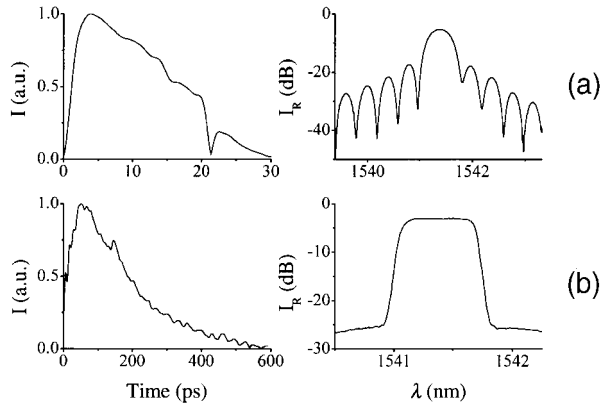

Fig. 3. Experimental impulse response and the corresponding reflection spectra (a) of a nearly uniform grating and (b) of a linearly chirped grating used for dispersion compensation.

speed of the measurement can be significantly reduced by use of a spectrum analyzer based on a grating and an array of detectors.

Because fiber gratings are linear devices, they can be analyzed by use of the impulse response of the grating for the reflected wave, $h(t)$.[12] Assuming that $e(t)$ is the amplitude of the pulses generated by the laser and that R is the coupling ratio of the fiber coupler, the field at the spectrum analyzer input equals $e_r(t) = R^{1/2}(1 - R)^{1/2}[e(t - \tau_0) + e(t) * h(t)]$, where τ_0 is the average delay between the arrival times of the pulse reflected by the grating and the pulse reflected by the mirror and $*$ is a convolution operator. The output of the spectrum analyzer is proportional to the time average of the spectrum intensity, $\langle I(\omega)\rangle = T\langle|E(\omega)|^2\rangle[1 + |H(\omega)|^2 + H(\omega)\exp(i\omega\tau_0) + \text{c.c.}] * H_s(\omega)$, where $H(\omega)$ and $E(\omega)$ are the Fourier transforms of $h(t)$ and $e(t)$, respectively, $H_s(\omega)$ is the response function of the spectrum analyzer caused by the analyzer's finite resolution, $T = R(1 - R)$, and $\langle\,\rangle$ denotes an average over a time period greater than the pulse duration. The inverse Fourier transform of the interference spectrum gives

$$p(t) = T[C_e(t) + C_e(t) * h(t) * h^*(-t) + C_e(t) * h(t - \tau_0) + C_e(t) * h^*(-t - \tau_0)]h_s(t), \quad (1)$$

where $h_s(t)$ and $p(t)$ are the inverse transforms of $H_s(\omega)$ and $\langle I(\omega)\rangle$, respectively, and $C_e(t) = \langle e(t) * e^*(-t)\rangle$ is the autocorrelation function of the input pulse. The third and fourth terms in Eq. (1) contain information on the impulse response of the grating. When autocorrelation function $C_e(t)$ is significantly narrower than the impulse response of the grating, the third and the fourth terms in Eq. (1) are approximately equal to the impulse response function $h(t)$ centered about $t = \pm\tau_0$. The first two terms in Eq. (1) are centered about $t = 0$ and can be filtered out when delay τ_0 is greater than the duration of the autocorrelation function of the impulse response, $h(t) * h^*(-t)$.

The time resolution of the impulse response is determined by the width of the autocorrelation trace, $C_e(t)$. In our experiment the effective bandwidth of the measurement was limited to $\sim\Delta\lambda = 20$ nm owing to the sensitivity of the spectrum analyzer. Assuming a spectrum with a Gaussian line shape, the time resolution of our system equals $\delta t = 4\ln(2)\lambda_0^2/\pi c\Delta\lambda = 350$ fs, where λ_0 is the central wavelength and c is the velocity of light. This time resolution, δt, corresponds to a spatial resolution of 37 μm. The maximum grating length that could be measured equals $L_{\max} = 2\ln(2)\lambda_0^2/\pi n\delta\lambda$, where $\delta\lambda$ is the resolution of our spectrum analyzer and n is the refractive index. According to the specifications of our spectrum analyzer the resolution is $\delta\lambda = 0.015$ nm and therefore the maximum grating length is 4.8 cm. In practice, we could measure lengths up to $\sim$7 cm.

Figure 3 shows the experimental impulse responses and the reflection spectra, obtained when the reference beam was blocked, for a nearly uniform fiber grating written with an UV laser and a phase mask [Fig. 3(a)] and for a chirped grating [Fig. 3(b)]. We note that the fluctuations in the impulse response of the chirped grating are caused by the grating structure and not by noise. The shape of the impulse response did not change from one measurement to another.

The impulse response of a grating gives the grating structure directly only when the reflection from the grating is weak.[13] In a strongly reflecting grating the impulse response does not directly give the grating structure because photons are multiply scattered and because the coherence properties of the pulse are destroyed as the pulse propagates inside the grating owing to the reflection of part of the frequency components by the grating. Therefore the impulse response cannot be directly used to extract the profile of the grating, and it can be used only to extract some parameters of the grating such as its magnitude and length, assuming that the grating profile is known.[3] We used the Gabor transformation[14] to extract directly some important information on the grating structure without the need to use complex and time-consuming calculations based on inverse scattering theory.[13] We have also developed a simple iterative method for extracting the refractive-index profiles of gratings with moderate reflections.[14]

The Gabor transformation of interference spectrum $I(\omega)$ is $G(t,\Omega) = \int_{-\infty}^{\infty} I(\omega)W(\omega - \Omega)\exp(-i\omega t)\mathrm{d}\omega$, where $W(\omega - \Omega)$ is a window function centered at frequency Ω. When the window function is narrower

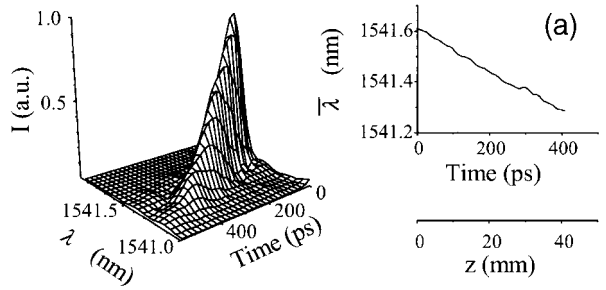

Fig. 4. Gabor transformation of the interference spectra measured for the chirped grating shown in Fig. 3(b), and dependence of the resonance wavelength of the grating on the location calculated from the Gabor transform. A Gaussian window with a width of 0.1 nm was used in the calculations.

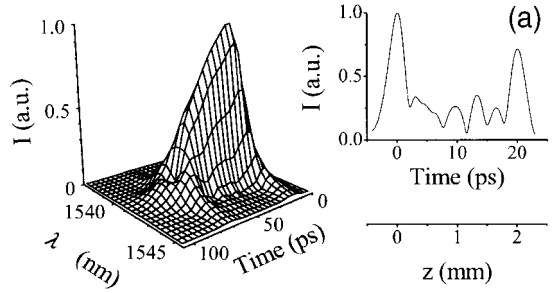

Fig. 5. Gabor transformation of the interference spectra measured for the nearly uniform grating shown in Fig. 3(a), and the cross section at $\lambda = 1545$. A Gaussian window with a width of 3 nm was used in the calculations.

than the bandwidth of spectrum $I(\omega)$, Gabor transform $G(t, \Omega)$ gives the time response of the grating for pulses with a spectrum $W(\omega - \Omega)$ centered at a frequency Ω. Figure 4 shows the results of the Gabor transformation for a chirped grating used for dispersion compensation. The window function had a Gaussian line shape with a bandwidth of 0.1 nm. Figure 4(a) shows the dependence of the average wavelength of reflected wave $\bar{\lambda} = \int_{-\infty}^{\infty} \lambda G(z = tc/2n, \lambda)\mathrm{d}\lambda / \int_{-\infty}^{\infty} G(z = tc/2n, \lambda)\mathrm{d}\lambda$ on the location inside the grating, z, assuming that the arrival time, t, and the location are linearly connected: $z = tc/2n$. The result of Fig. 4 shows that the resonance wavelength of the grating depends linearly on location z, as expected for a linearly chirped grating. The slope of the change in the resonance wavelength is ~1190 ps/nm, in accordance with the specified group-velocity dispersion for that grating, 1120 ps/nm. The small difference between the results is caused at least in part because the reflection from each region inside the grating has a finite bandwidth and therefore each region can reflect frequency components that are slightly different from its resonance frequency.

Figure 5 shows the Gabor transformation for a nearly uniform grating and its cross section at a wavelength $\lambda = c/\Omega = 1545$ nm located far outside the central wavelength of the Bragg zone, $\lambda_0 = 1541.5$ nm. The window function had a Gaussian line shape with a bandwidth of 3 nm. This figure and theoretical analysis indicate that pulses with frequency components outside the Bragg zone are strongly reflected only from nonuniform regions of the grating, such as the boundaries. Nonuniform regions of the grating can be considered thin gratings with broad reflection spectra. Therefore such regions can strongly reflect frequency components located far outside the Bragg zone of the whole grating. The two strongest peaks shown in Fig. 5 are caused by the boundaries of the grating. The distance between those peaks, 2 mm, is in accordance with the size of the slit used during writing of the grating, 2 mm. Our theoretical analysis indicates that the Fresnel reflection caused by changes in the average refractive index at the boundaries is negligible in our grating, since this reflection is obtained from an interface, whereas the reflection from the grating is obtained from a finite section of the fiber.

In conclusion, we have developed a simple method for obtaining the impulse response of fiber Bragg gratings, based on low-coherence spectral interferometry of noiselike pulses. Our method requires a single pulse for interrogation of the whole grating. Using Gabor transformation, we directly obtained important information on the structure of the grating.

We thank Y. Zeevi for stimulating discussions. This research is supported by the Division for Research Funds of the Israeli Ministry of Science. M. Horowitz's e-mail address is eermoshe@ee.technion.ac.il.

References

1. C. R. Giles, J. Lightwave Technol. **15,** 1391 (1997).
2. D. Sandel, R. Noè, G. Heise, and B. Borchert, J. Lightwave Technol. **16,** 2435 (1998).
3. P. Lambelet, P. Y. Fonjallaz, H. G. Limberger, R. P. Salathé, Ch. Zimmer, and H. H. Gilgen, Photon. Technol. Lett. **5,** 565 (1993).
4. E. I. Petermann, J. Skaar, B. E. Sahlgren, R. A. H. Stubbe, and A. T. Friberg, J. Lightwave Technol. **17,** 2371 (1999).
5. R. Trebino and D. J. Kane, J. Opt. Soc. Am. A **10,** 1101 (1993).
6. D. Meshulach, D. Yelin, and Y. Silberberg, J. Opt. Soc. Am. B **14,** 2095 (1997).
7. T. Funaba, N. Tanno, and H. Ito, Appl. Opt. **36,** 8919 (1997).
8. M. Horowitz, Y. Barad, and Y. Silberberg, Opt. Lett. **22,** 799 (1997).
9. M. Horowitz and Y. Silberberg, IEEE Photon. Technol. Lett. **10,** 1389 (1998).
10. M. N. Putnam, M. L. Dennis, I. N. Dulling III, C. G. Ashkin, and E. J. Friebele, Opt. Lett. **23,** 138 (1998).
11. J. U. Kang and R. Posey, Opt. Lett. **23,** 1375 (1998).
12. J. Shamir, *Optical Systems and Processes* (SPIE, Bellingham, Wash., 1999), p. 28.
13. E. Peral, J. Capmany, and J. Marti, IEEE J. Quantum Electron. **32,** 2078 (1998).
14. D. Gabor, J. Inst. Electr. Eng. **93, Part 3**, 429 (1946).
15. S. Keren and M. Horowitz, in *Conference on Lasers and Electro-Optics*, 2000 OSA Technical Digest Series (Optical Society of America, Washington, D.C., 2000), p. 433.